



Contents lists available at ScienceDirect

Computer Communications

journal homepage: www.elsevier.com/locate/comcom

A cross-layer adaptive mechanism for low-power wireless personal area networks

Selcuk Okdem*

Erciyes University, Engineering Faculty, Computer Engineering Department, Kayseri, Turkey

ARTICLE INFO

Article history:

Received 15 May 2015

Revised 6 November 2015

Accepted 8 November 2015

Available online xxx

Keywords:

Cross-layer communication

IEEE 802.15.4-based protocols

Wireless personal area networks

ABSTRACT

This article presents a novel method providing reliable data links for low-power wireless personal area networks. The method implements a dynamic frame formation using hamming-codes. The formation process is made in an optimum way to obtain high throughput while questioning channel condition in the network. A cross-layer interaction is utilized to get noise resilient link layer operations. This interaction is achieved by querying the value of bit error rate from the physical layer. The method is adapted to be used in low-power and low-rate wireless networks based on IEEE 802.15.4 protocol. Performance metrics are evaluated through extensive Monte Carlo simulations and its success is compared to IEEE 802.15.4 and IEEE 802.15.4g protocol outputs. The simulations are made over various communication types using high traffic loads. In all our experiments, the proposed method substantially increases communication throughput, reduces energy consumption, and increases network life-time.

© 2015 Elsevier B.V. All rights reserved.

1. Introduction

Low-power, low-rate wireless communications have received a lot of attention in the recent years. This type of communications has a wide range of application areas including Wireless Personal Area Networks (WPANs), Wireless Sensor Networks (WSNs), and various industrial control systems. Although these systems need low-power and low-cost hardware while presenting higher flexibility, a number of physical factors influence the communication efficiency. These factors include limited communication range, vulnerability to environmental noise signals, and higher signal fading for mobile communications. All of these factors cause unreliable links which eventually degrade the system performance.

Forward Error Correction (FEC) and Direct-Sequence Spread Spectrum (DSSS) methods are commonly used in wireless communications. The first one provides error control in data transmission over noisy communication channels. However, the second one utilizes spreading techniques for the purposes of establishment of a secure communication, increasing resistance to natural interference, and environmental noise. DSSS is also used to provide multiple communications over a single channel by Code Division Multiple Access (CDMA). Both of the methods improve the link reliability by means of redundant information in the original data. By means of FEC, this redundancy helps receiver nodes correct erroneous bits. On the other hand,

DSSS utilizes this redundancy to provide more robust communications in noisy environments. A binary data string, received by radio circuitry, may have erroneous bits caused by noise signals. Bit error rate gives information about the amount of erroneous bits in the string. FEC and DSSS methods are characterized by their code ratios, and spreading factors, respectively. It is desired to get high performance while using little redundancy data which means providing big code ratio and small spreading factor [1].

IEEE 802.15.4 is a commonly used protocol in WPANs, WSNs, and industrial control systems [2,3]. The protocol can be used with 6LoWPAN [4] and upper-layer internet protocols to build wireless embedded internet. It is organized to be operated in low-power, low-rate communications in noisy environments. Its initial version (named as IEEE 802.15.4) uses DSSS process which encodes 4-bits messages to 32-bits strings as chip sequences on transmission, and decodes vice versa on reception. The mechanism has a spreading factor of $32/4 = 8$, and provides a high noise resilient message transmission process. A new version of IEEE 802.15.4 (named as IEEE 802.15.4g-2012) uses both FEC and DSSS processes which provide an improved noise resilient operation. A large number of analytical and simulation studies have been made on the performance of IEEE 802.15.4 protocol. A detailed research on the performance analysis is made by Misis et al. [5]. This analysis includes the performance results on Media Access Control (MAC) related parameters such as packet transmission and loss rate. It is modelled by probability based functions and the results are illustrated thoroughly. Although their paper presents a detailed information about the protocol performance, there is no research on the effect of different FEC coding strategies. Zhu et al. made

* Tel.: +90 3522076666.

E-mail address: okdem@erciyes.edu.tr, slckokdem@gmail.com

Table 1
Performance analysis in the references.

Analysis	[3]	[4]	[5]	[6]	[7]	[8]	[9]	[10]	[11]
PHY layer	–	–	✓	✓	✓	✓	✓	–	–
MAC layer	✓	✓	✓	–	–	–	–	–	–
Cross-layer operation	–	–	–	–	–	–	–	✓	✓
Mobile conditions	–	–	–	–	–	–	–	–	–
BCH coding	–	–	–	–	✓	–	–	–	–
LDPC coding	–	–	–	–	–	✓	✓	–	–
IEEE 802.15.4 coding	–	✓	✓	✓	–	–	–	–	–
IEEE 802.15.4g coding	✓	–	–	–	–	–	–	–	–

another investigation about the protocol performance [6]. However, their study deals with only unsaturated network traffic without considering the effect of FEC coding. Shen and Abedi introduced a new method about using Bose, Chaudhuri, and Hocquenghem (BCH) coding [7]. They analysed the effect of BCH coding as a FEC strategy on bit error rate performance. Their paper covers only physical layer operations, and MAC related co-operations are not studied to improve the link-layer performance. A different code adaptation scheme which employs LDPC (Low-Density Parity-Check) codes is proposed in [8]. This study aims an energy efficient communication in WSNs by reducing bit errors. A similar study [9] is made about LDPC coding for Wireless Body Area Networks (WBANs). However, these studies have no research on the effect of dynamically changing bit error rates which occur at mobile conditions at run-time. They deal with only physical layer performance issues by lowering bit error rates. No link layer performance issue is evaluated, and no cross-layer cooperation is established. To address the performance issues on link layer protocols using cross-layer cooperation, several proposals have been made as in [10,11]. Although these proposals provide strong scheduling mechanisms, flow controls, and clock synchronizations, no research has been made to analyse the effect of noise signals on the link layer performance. Table 1 gives a brief comparison to summarize the related work. Various coding methods are used by the references in the table including IEEE 802.15.4 PHY, IEEE 802.15.4g PHY, BCH(15,7) and LDPC coding. The first coding method, IEEE 802.15.4 PHY, has a common usage in both of research and industrial purposes [4–6]. However, an improved version of this method, IEEE 802.15.4g PHY [3], is developed to enhance and add functionality to the IEEE 802.15.4 PHY and MAC to better support the industrial markets. Performance improvement by this new coding method is analysed in Section 5. In order to decrease bit error rate, other PHY coding methods such as BCH and LDPC are used by authors of [7–9]. Although they utilized IEEE 802.15.4 MAC functionalities, coding with BCH and LDPC methods is achieved instead of standard IEEE 802.15.4 PHY coding. They focused on developing hardware components and their complexity issues. Although, they made performance analysis about bit error rate in PHY layer, they included no link layer analysis. Other studies such as in [10,11] propose upper-layer communication methods using multi-hop data transfer. Although, these methods offer suitable solutions for IEEE 802.15.4 based networks (specifically highly populated networks as in WSNs), their applications are unavailable for a single hop local area networks such as WPANs.

With regards to cross-layer techniques, queries about link quality and bit errors provide a valuable information to adapt the parameters of error correcting methods and link layer algorithms. This cross-layer approach improves link performance in respect of data throughput and packet delivery ratio. In this work, we are motivated by the observation that mobile condition (changes in the communicating distance) leads changes in received signal strength and bit error rate. It is possible to organize MAC frames to get a better performance for this kind of dynamic topology. Such an approach makes it possible to design more resilient communication scheme for noisy environments. More specifically, we propose a novel cross-layer mechanism

of physical to/from link layer for low-rate, low-power devices in mobile conditions. To the best of our knowledge, it is the first time that organizing MAC frames for low-power WPANs according to different values of bit error rate. The novelty and contributions presented in this paper are summarized as follows:

- A cross-layer method for MAC frame organization is proposed. This organization provides a highly noise resilient data communication scheme.
- An adaptive link-layer operation is proposed for mobile conditions.
- A more robust communication scheme is made providing energy efficient operations for battery powered LR-WPAN networks.

This paper is divided into six sections: in Section 2, IEEE 802.15.4 and IEEE 802.15.4g protocols are given in brief. Sections 3 and 4 explain our model by introducing its MAC frame organization and wireless operation. Section 5 includes experimental results to illustrate the model performance, and finally Section 6 concludes the paper.

2. IEEE 802.15.4 and IEEE 802.15.4g protocols

IEEE 802.15.4 and IEEE 802.15.4g protocols provide PHY and link layer functionality for WPANs. These protocols are standardized by IEEE P802.15 Working Group. IEEE 802.15.4 is an initial version of low-rate WPAN protocol family and IEEE 802.15.4g is a specialized version of its counterpart developed in 2003 and 2012, respectively.

PHY layers of IEEE 802.15.4 and IEEE 802.15.4g operate in many different frequency ranges. Operation in 2450 MHz is a popular range for these protocols that offers 2 Mchip/s transmission capability by Offset Quadrature Phase-Shift Keying (O-QPSK) modulation. 16 communication channels are available for this range and each channel has 5 MHz wide. Each packet in 2450 MHz operation begins with a preamble sequence (PRE), Synchronization header (SYN), and a PHY header. These fields are followed by a variable length of payload. The lengths are limited to 127 octets for IEEE 802.15.4 and 2047 octets for IEEE 802.15.4g. Because an IPv6 packet has a minimum of 1280 octets, an adaptation protocol of 6LoWPAN is used for IEEE 802.15.4 to enable IPv6 internet usage [12]. Apart from frame lengths, other differences between IEEE 802.15.4 and IEEE 802.15.4g rely on PHY layer. The alternate PHYs of IEEE 802.15.4g support outdoor, low-rate, smart metering utility network (SUN) applications under multiple regulatory domains. The SUN PHYs include multi-rate and multi-regional frequency shift keying (MR-FSK), multi-rate and multi-regional orthogonal frequency division multiplexing (MR-OFDM), and multi-rate and multi-regional offset quadrature phase-shift keying (MR-O-QPSK) modulations. The PHY layer of SUN supports multiple data rates in bands ranging from 169 MHz to 2450 MHz. While DSSS operation is compulsory in IEEE 802.15.4, it is optional in IEEE 802.15.4g according to the option of packet type. Although SHR and PHR fields are transmitted by means of DSSS operations, PSDU field can be transmitted in three ways in IEEE 802.15.4g using mode 0, mode 1, or mode 2 as shown in Fig. 1. As seen from the figure, mode 2 has no DSSS operation. Transmissions of PHR and PSDU fields are also exposed to an FEC

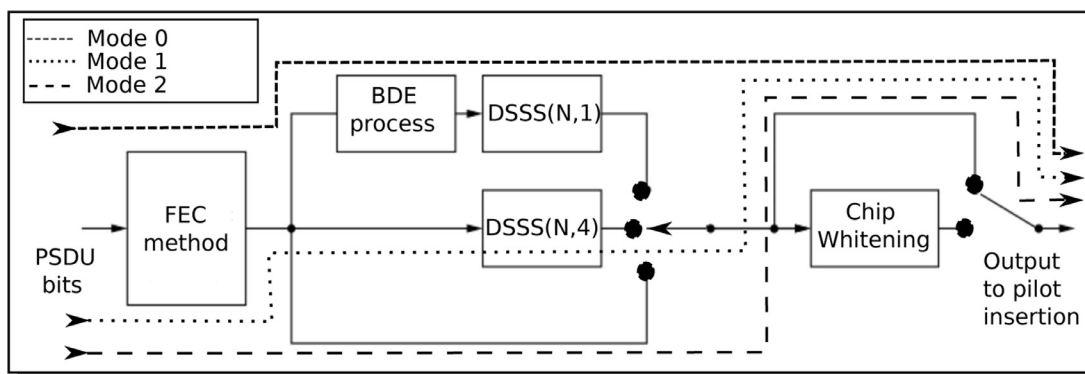


Fig. 1. IEEE 802.15.4g PSDU transmission modes [3].

operation with a rate of 1/2 convolutional coding using the generator polynomials given by G_0 and G_1 in Eq. (1). Bit differential encoding (BDE) operation is an optional operation according to transmission mode as described in Eq. (2) where $R(n)$, $E(n)$, and $E(n - 1)$ denote the raw bit being encoded, corresponding differentially encoded bit, and the previous differential encoded bit, respectively. This equation simply makes a modulo-2 operation of raw bit with the previous encoded bit. Although IEEE 802.15.4g has options for DSSS, FEC, and BDE operations, IEEE 802.15.4 has no utility for FEC and BDE operations.

$$G_0(x) = 1 + x^2 + x^3 + x^5 + x^6,$$

$$G_1(x) = 1 + x + x^2 + x^3 + x^6. \tag{1}$$

$$E(n) = R(n) \oplus E(n - 1). \tag{2}$$

In IEEE 802.15.4 and IEEE 802.15.4g, CSMA/CA algorithm is used to access physical medium for unslotted operations. The flowchart of the operation is given in Fig. 2. As a first step of the transmission, NB (number of trials to access to the channel) and BE (back-off exponent) are set to 0 and $macMinBE$ (minimum back-off period), respectively. After a random number of back-off periods in $(2^{BE}-1)$ slots, channel condition is evaluated for the transmission. If it is sensed as idle for two subsequent access', the packet is issued to transmission process. After receiving the packet successfully, destination node transmits an acknowledgement packet (ACK). If the channel is sensed busy before the transmission, then NB is incremented by 1. This process can be repeated at most M (defined as $macMaxCSMABackoffs$) times. After an ACK is received in $MacAckWaitDuration$ then the transmission is considered as being successful. Otherwise, transmission process is restarted. Default parameter values of NB , BE , $macMinBE$, M , and $MacAckWaitDuration$ are given in related protocol specifications [2,3].

2.1. FEC and DSSS methods used in IEEE 802.15.4 and IEEE 802.15.4g protocols

Initial version of IEEE 802.15.4 protocol uses only a DSSS method. However, current version of the protocol utilises both of these methods. Data rate of an IEEE 802.15.4 compliant device is limited with its hardware capability. This limit is defined as 2 Mchip/s in protocol specifications [2,3]. In the paper, the notation of “chip/s” is used to express transmission rate after coding (by FEC) and spreading (by DSSS) as processes are switched to PHY layer operations. Data rate is not only constrained by transceiver hardware but also by FEC and DSSS methods. The ratio of input bits to output bits of a FEC method is called as code rate. Since, output of the device is limited with 2 Mchip/s, a FEC method with 1/2 code rate causes data rate to decrease to 1 Mbit/s. Spreading factor of a DSSS method has also a similar effect. Initial version of IEEE 802.15.4 protocol uses a spreading factor of 8 owing to DSSS(32,4) which decreases the rate to 250 kbit/s with 2 Mchip/s transceiver hardware. However, IEEE 802.15.4g protocol does not use any DSSS method for the transmission of frame

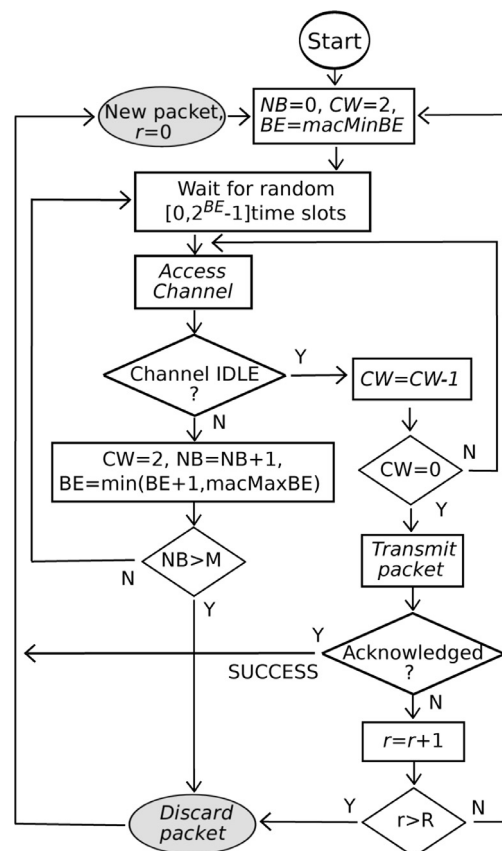


Fig. 2. Channel access flowchart of the protocols.

header. It utilise DSSS(8,4) for transmission of PSDU field in the frame with spreading factor 2, and a FEC method with 1/2 code rate which decreases the rate to 500 Kbit/s as defined in [3].

3. A proposal for Adaptive Data Link Layer operations

A mechanism for Adaptive Data Link Layer (ADLL) operations can improve the link layer performance over noisy channels. In our proposal, it is aimed to get efficient wireless operations for low-rate and low-power communications. For the purpose of PHY layer compliance, the same configuration and control fields are used as in IEEE 802.15.4g. The fields include seven PHY and MAC headers and 32-bits cyclic redundancy check (CRC) trailer for 2.4 GHz MR-O-QPSK operations in short addressing without coordinator mode. Header control fields and their lengths are given in Table 2. Payload is

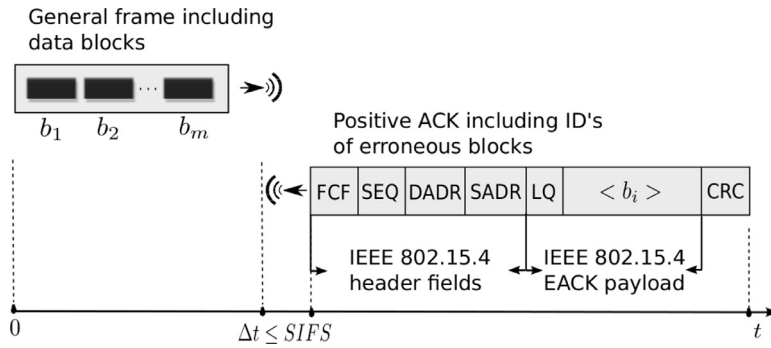


Fig. 3. Transferring data blocks.

Table 2
Header fields.

Name	Description	Length
PRE	Preamble bits	56-bits
SDF	Start of frame delimiter	16-bits
PHR	PHY header	24-bits
FCF	Frame control field	16-bits
SEQ	Sequence number	8-bits
DADR	Destination address	16-bits
SADR	Source address	16-bits
LQ	Link quality	16-bits
CRC	Cyclic redundancy check	32-bits

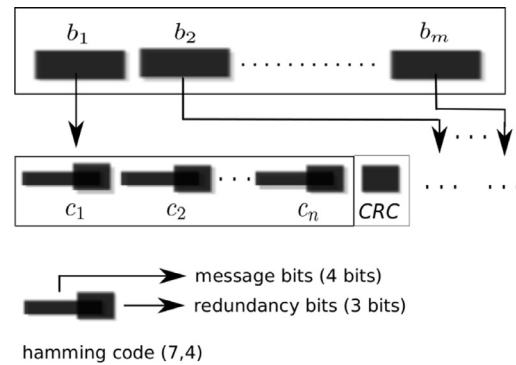


Fig. 4. Data blocks and their contents.

appended just after the header fields as shown in Fig. 3. In general frame, MAC header fields (FCF, SEQ, DADR, SADR) are included in data blocks as well as MAC payload. ADLL uses the same FEC and DSSS methods for the PHY header control fields (PRE, SDF, and PHR). However, it uses a different error correction mechanism for MAC fields (which are composed of data blocks). This mechanism utilizes hamming codes. It splits MAC header and payload into m data blocks (each of them includes n hamming codes). Any single error in these codes can be corrected by means of hamming decoder. These corrections provide no data retransmission procedure. Only erroneous data blocks (whose IDs are placed in ACK frame) are retransmitted. Acknowledge frame includes the same header fields as general data frames. It also includes the field of LQ, erroneous block IDs ($\langle b_i \rangle$), and a CRC field. These fields are not issued in IEEE 802.15.4g. However, ADLL utilizes the field of payload (named as EACK) of IEEE 802.15.4g to place LQ, $\langle b_i \rangle$, and CRC fields. The frames are formatted as illustrated in Fig. 3. Error detection process for header fields is made by means of CRC field. Erroneous blocks, that cannot be corrected by hamming decoder in complete, are detected by their individual CRC fields. IDs of these blocks constitute of $\langle b_i \rangle$. The size of blocks is adjusted to an optimum value by Algorithm 1 as explained in Section 4. The algorithm searches the

Algorithm 1 Calculate the optimum sizes of blocks.

```

bitErrorRates  $\leftarrow$  linearly distributed  $n$  values in  $[0, 0.5]$ 
for all  $i$  such that  $1 \leq i \leq n$  do
   $\rho \leftarrow$  bitErrorRates $_i$ ; maxRate $_i \leftarrow 0$ 
  for all  $j$  such that  $1 \leq j \leq m$  do
    rate $_{ij} \leftarrow \frac{4}{7} \cdot \frac{j}{j+5} \cdot (1-\rho)^5 \cdot [(1-\rho)^7 + 7 \cdot \rho \cdot (1-\rho)^6]^j$ 
    if maxRate $_i <$  rate $_{ij}$  then
      maxRate $_i \leftarrow$  rate $_{ij}$ 
      optimumNumber $_i \leftarrow j$ 
    end if
  end for
end for

```

optimum data size in the range of $[1, 32]$ bytes. The CRC's attached to the blocks are calculated by CRC-8 algorithm.

The field of FCF contains information about the frame type and control flags as used in IEEE 802.15.4g. Although the same control configuration can be used with ADLL, some exceptions are in issue. The first exception is that its addressing method supports only 16-bits identification. The second exception resides on the spreading process. In contrast to IEEE 802.15.4g operations, ADLL does not utilize any spreading method.

Data blocks are considered as sub-blocks of a frame which is split into m parts numbered from b_1 to b_m as given in Fig. 4. At the beginning of the transmission, n (the number of codes) is set to minimum value (which is 1). After getting ACK messages, this value is set to an optimum value obtained by data link layer calculations. These calculations are made according to the value of LQ field of ACK. This field is updated by the destination node and includes the value of link quality. This quality value is calculated by the inverse ratio of bit error rate and scaled to the nearest integer value in $[0, 255]$. Bit error rate is queried from PHY layer where data link and PHY layer interaction is evaluated as a cross-layer operation.

4. ADLL operation in wireless networks

As discussed in Section 2.1, FEC and DSSS methods can correct errors using code redundancy. Code ratio of a FEC method gives information about the inverse ratio of the redundancy level, where it is given by the ratio of input bits to output bits. However, redundancy level of a DSSS is expressed by its spreading factor where it is given by the ratio of output bits to input bits. For a given chip rate (2 Mchip/s for IEEE 802.15.4 based devices), data rate is found by Eq. (3) where t , c , ω , and f represent data rate, code rate, spreading factor, and chip rate (supported by the transceiver hardware), respectively,

$$t = c \cdot \frac{1}{\omega} \cdot f. \quad (3)$$

Table 3
Data rates of IEEE 802.15.4g PHY fields.

PHY field	c	ω	t
SHR	–	128	$(1/128) \cdot f$
PHR	1/2	32	$(1/64) \cdot f$
PSDU	1/2	2	$(1/4) \cdot f$

Table 4
Data rates of IEEE 802.15.4 PHY fields.

PHY field	c	ω	t
SHR, PHR, and PSDU	–	8	$(1/8) \cdot f$

Table 5
Data-bits and corresponding hamming codes (LSB first).

Data-bits	Hamming codes	Data-bits	Hamming codes
0000	0000000	0001	1010001
1000	1101000	1001	0111001
0100	0110100	0101	1100101
1100	1011100	1101	0001101
0010	1110010	0011	0100011
1010	0011010	1011	1001011
0110	1000110	0111	0010111
1110	0101110	1111	1111111

ADLL uses the same FEC and DSSS processes as in IEEE 802.15.4g for header transmission. Bits of SHR (synchronization header) and PHR (PHY header) are coded/spread in a way that results $f/128$ and $f/64$ data rate as given in Table 3 where PSDU constitutes PHY service data unit. Difference in ADLL's operational behaviour relies on PSDU transmission. Although IEEE 802.15.4g uses FEC with code rate of 1/2 and DSSS with spreading factor of 2 (Table 3), ADLL uses only FEC process with code rate of 4/7. However, IEEE 802.15.4 uses only DSSS process with spreading factor of 8 as given in Table 4. Although IEEE 802.15.4 provides a robust noise resilient coding functionality, low data throughput is expected due to its high spreading factor.

Data in PSDU field is split to form data blocks which include hamming codes with 7 code-bits and 4 data-bits in an ADLL communication. This process results the value of code rate as 4/7. Data-bits and their corresponding hamming codes are given in Table 5. Hamming codes can detect up to 2-bit errors or correct 1-bit error. Since these codes achieve the highest possible code rate with their block length and minimum distance 3, they are called as perfect codes [13]. A tracking mechanism is achieved by the receiver to record erroneous data blocks. By means of this information, these blocks are requested to be retransmitted by including their IDs in ACK field. In IEEE 802.15.4 and IEEE 802.15.4g protocol operations, whole data is retransmitted in case of an error. This unnecessary data traffic is eliminated by ADLL's tracking mechanism. Data splits and erroneous block IDs are placed in the frames as shown in Fig. 3.

ADLL's transmission begins with M (valued as 56 for MR-O-QPSK) preamble bits, all zero, and 16-bits delimiter indicating frame start which is valued by [1110101101100010] in binary. This sequence, including preamble and delimiter bits, constitutes the field of SHR. Before transmission, two processes are applied to SHR bits. The first process is bit differential encoding (BDE) described as in Eq. (2), and the second process is $(N,1)$ -DSSS where N is valued by 128. $(N,1)$ -DSSS bit mapping can be found in [3]. After transmission of SHR bits, 24 bits of PHR are transmitted. PHR is also exposed to the processes of BDE and $(N,1)$ -DSSS where N is valued by 32. It is also processed by FEC before these two operations. This FEC mechanism uses two generator polynomials, which are given in Eq. (1) resulting two outputs per one input. These transmission procedures for SHR and PHR are the same as in IEEE 802.15.4g.

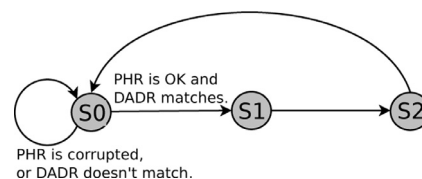


Fig. 5. State diagram of the proposed link layer algorithm.

Table 6
Operation steps of the states.

Name	Operation steps
S0	Receive frame, check PHR field, decode addresses, and check if it matches to DADR
S1	Receive data blocks, decode them (using hamming decoder), calculate block CRCs and check them, identify erroneous blocks, and get their ID's to form (b_i)
S3	Send acknowledge frame, forward decoded data (possibly corrected) to upper layer, and return to state S0

Payload data is transmitted in PSDU field. In IEEE 802.15.4g, this field is firstly processed by FEC mechanism explained above, then interleaved to take a preventive measure for bursty errors, and finally processed by $(N,4)$ -DSSS where N is valued by 32. However, ADLL uses a different kind of FEC mechanism illustrated in Fig. 4, and no DSSS process. The FEC mechanism works in an adaptive manner by adjusting the values of m and n at run-time. However, the same interleaver process is used as in IEEE 802.15.4g.

To analyse the effect of block sizes, let ζ denote the probability of getting erroneous code that cannot be corrected. Due to the fact that a hamming decoder of 7 code and 4 data bits can correct 1 possible erroneous bit, a successful transmission of 7-bits hamming code can be seen at the probability value which is calculated by Eq. (4). This equation states that success of probability is the probability of that seven bits are correct or only one bit is erroneous,

$$\zeta = (1 - \rho)^7 + 7 \cdot \rho \cdot (1 - \rho)^6. \quad (4)$$

Consider a block with the parameters of n (number of codes) and s (number of CRC bits), then Eq. (5) states the probability of providing error-free transmission for a block,

$$P = (1 - \rho)^s \cdot \zeta^n, \\ = (1 - \rho)^s \cdot [(1 - \rho)^7 + 7 \cdot \rho \cdot (1 - \rho)^6]^n. \quad (5)$$

Then, transfer rate (the ratio of successfully received data bits) is calculated by Eq. (6). The factor of 4/7 is used because 7-bits hamming code includes 4-bits message data. Since n bits data is accompanied by s bits CRC, the ratio of $n/(n+s)$ is another factor included in the equation,

$$r = \frac{4}{7} \cdot \frac{n}{n+s} \cdot P \quad (6)$$

Because the number of n has influence on the probability of block errors as seen in Eq. (5), it is essential to find the optimum value of n . For a given set of ρ , the best value of n for each value of ρ can be found by a searching method. The algorithm, used to find the best number, is given in Algorithm 1. In the algorithm, optimum block sizes are calculated for a set of bit error rates. Results are obtained in the array of *optimumNumber* including optimum numbers of hamming codes in the block, providing the best transfer ratio.

In the reception process, three states are utilized. Execution of the states is made conditionally. Fig. 5 shows the states and switching conditions. Note that switching from S1 to S2, and S2 to S3 has no condition. Descriptions of the states are given in Table 6.

4.1. Deriving a light-weight function for the optimum block size

Transmission with minimal error is an important factor on the quality of link layer operation. To provide successful transmissions at a high rate, ADLL searches for the optimum value of n . This value is defined as *optimumNumber* in Algorithm 1. For a given ρ value in the range of [0,0.5], this optimum value can be found by Algorithm 1. However, the search process employed by the algorithm brings a high degree of complexity including many iterations of calculations using Eq. (6). Such a complexity can cause some implementation problems for low-power WPANs having limited processor capabilities and low-capacity memories.

A real-time function in a low complexity manner can produce the optimum value of n . Since this process is executed in a single step, it is expected that run-time is decreased considerably. In this sense, the function given in Eq. (7) can be used to obtain the value of n for a given ρ . The function is characterized by its parameter set given as \bar{a} .

$$n = f(\bar{a}, \rho). \quad (7)$$

Algorithm 1 utilizes the outputs of the function given by Eq. (7). It is used to get \bar{a} by means of an interpolation method. In order to obtain a functional fit through the data obtained by the algorithm, the sum of the squares of the differences between the actual data and function fit is evaluated. This evaluation is made by a popular optimization method named Levenberg–Marquardt [14]. Although several other optimization methods can offer similar results, Levenberg–Marquardt method is preferred due to its fast convergence characteristic.

ADLL uses this fit in real-time to adjust its block sizes given in Fig. 4 to an optimum level. It is not possible to observe ρ as stable in a mobile environment, since the channel has varying signal to noise ratio according to the changes in communication distances. So, it is required to adjust the sizes according to the current channel condition. The steps for the adjusting process are below:

- Step 1. Query the current value of ρ from PHY layer.
- Step 2. Calculate the value of n using Eq. (7).
- Step 3. Adjust block sizes to n .

The usage of the method and the process of the functional fit through the experimental data are described in Section 5.

4.2. Suitability of ADLL for IPv6

IP connectivity with IPv6 over low-power WPANs allows electronic devices with low-power and limited hardware to connect to internet. Since low-power WPAN devices use transmission signals at low strengths, transmitted packets are more vulnerable to noise signals. Moreover, frame error rate is observed at high values for larger frame sizes, since a large packet is more prone to errors than the smaller one. Therefore, initial versions of IEEE 802.15.4 protocol use 127 octets of maximum frame size which is relatively too smaller than the sizes of other IEEE wireless communication protocols. Transmissions of IPv6 Packets over IEEE 802.15.4 networks using 127 octets are made by 6LoWPAN standard [12]. This standard proposed by IETF to be used for internet connection of networks using low powered devices. Each device in this type of networks uses short range transmissions. A compression mechanism is introduced in the standard to reduce the overhead of IPv6 headers [15]. A fragmentation process is also provided by the standard. This is because an IEEE 802.15.4-2003 frame can get a maximum size of 127 octets (including 102 data octets). Although IEEE 802.15.4-2003 requires segmentation and re-assembly operations for 6LoWPAN, there is no need to achieve these operations for IEEE 802.15.4g and ADLL protocols. Because their frame lengths can easily be adapted to 1280 octets which is required minimum frame size for IPv6 packets.

Table 7
Coefficients of the function.

Function	a_0	a_1	R-square (%)
Eq. (8)	$4.06 \cdot 10^{-2}$	$1.26 \cdot 10^{-3}$	99

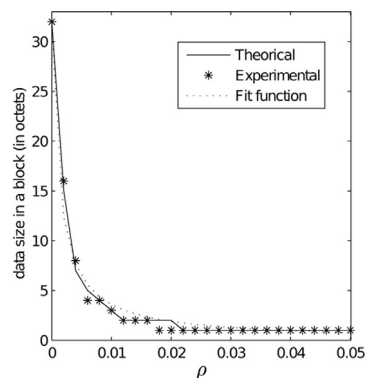


Fig. 6. Optimum number of codes.

Mobile communications are common in a large number of 6LoWPAN applications. Therefore, it is essential to maintain IP connectivity in mobile conditions. Mobility is the main factor causing signal strength to be changed according to communication distance. The change in the strength eventually results different ρ values. The quality of wireless communication is highly dependent on the value of ρ . Therefore, the mobility is the key factor effecting the performance of WPAN internet connections. ADLL can offer a superior success at this point than its counterparts. ADLL also offers a significant amount of overhead elimination for the adaptation layer of 6LoWPAN as well as IEEE 802.15.4g. This overhead is unavoidable for IEEE 802.15.4 communications. Such an overhead of segmentation at transmission stage, and reassembly at reception stage may cause long execution times for low-power devices with limited processor capability and memory capacity.

5. Performance results

The results presented in this section are experimentally obtained by running the scenarios 50 times providing 95% confidence interval which indicates the reliability of our measurements. We utilized a parallel discrete model providing continuous data transferring, which is developed in Octave.

In order to obtain optimum block sizes for the current environmental condition (with bit error rate of ρ), Algorithm 1 is used. However, it is a time consuming job for a real time process. Therefore, a lighter equivalent real time function is derived by means of curve fitting. Polynomial functions are among the most frequently used empirical models. However, they have poor interpolation properties, and high-degree polynomials cause oscillations between fit values. High-degree polynomials also require long processing times that is not suitable for real-time systems. Rational function models offer moderately simple forms. They accommodate much wider range of shapes than do the polynomials. They can often be used for modelling with lower degrees and fewer coefficients compared to the polynomial models [16]. Therefore, we prefer to use a light version of rational function.

Curve fitting process is made by a first degree rational function which is given in Eq. (8). The simplicity of this function offers a fast calculation. The process is made according to the steps explained in Section 4.1. After this process, coefficients of the function are obtained where the values of them are given in Table 7. Fig. 6 shows the results of theoretical (by Eq. (5)), experimental (by Monte Carlo

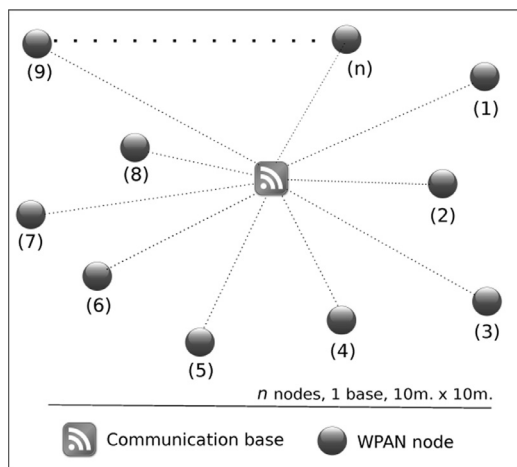


Fig. 7. Wireless personal area network used in the simulations.

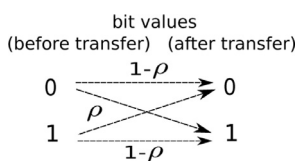


Fig. 8. A BSC process.

machine), and rational fit function of degree 1,

$$f = a_0 / (a_1 + x). \tag{8}$$

From the figure, it is seen that fit function closely follows the experimental and theoretical data. It successfully fitted with suitability degree of 99% (*R*-square).

The performance results of the protocols in a WPAN are obtained using an example network given in Fig. 7. This WPAN area includes a wireless router and a number of nodes representing wireless hosts such as mobile devices and internet of things. They are initially placed in random in a fixed area of (10 m × 10 m), and a single base located in the middle (5 m × 5 m). For performance measurements, authors of [12] and [5], assumed the number of nodes (denoted as *n*) as 10, and various values from 5 to 50, respectively. In our experimental scenario, this number is assumed as 5, 10, and 50 for small, moderate, and dense WPANs, respectively.

Binary Symmetric Channels (BSCs) are used in our experiments as wireless channels for physical-layer operations as in [17]. According to BSC model, each bit in a frame has the same probability (ρ) to be corrupted. This probability has no dependency on its previous values and previous erroneous situations. This process is simply illustrated

in Fig. 8. The choice of BSC is not required for our model but it simplifies performance analysis of the proposed link-layer method. Link-layer setup parameters are used as specified by their default values in [2,3]. These values are given in Table 8. Simulation setup also utilizes chip specific parameters (ADF7241) to follow a realistic setting [18]. The values of these parameters are given in Table 9. In simulations, it is assumed that every node has a capability of communicating with others. Free space radio model is used as discussed in [19], with energy consumption values on the receiver (E^{RX}) and the transmitter (E^{TX}). The values of E^{RX} and E^{TX} are experimentally found by measuring energy consumptions for transmission and reception, using the device where its chip specific parameter values are given in Table 9. The experiment includes a transmitter and a receiver with setup parameter values given in Table 8. The consumption values are obtained using physical-layer measurements. Output power of transmission amplifier is adjusted to the minimum level which provides enough power to keep receiver's Link Quality Indicator (LQI) on. LQI is referenced as the level which provides desired ρ values for 1Kbit data transfer. This adjustment is made for various ρ values and distances (open-air) to plot energy consumptions. Experimental data for E^{TX} is plotted in Fig. 9 where E^{RX} is measured as $2.75 \cdot 10^{-7}$ Joules.

A small sized lithium battery model suitable for low-power WPAN nodes which can supply about a 100 J is used [20]. Simulations are run until network energy is depleted to 10% which is expressed as Normalized Energy Level (NEL) in Figs. 18–23.

The performance evaluation considers two aspects: (i) network life-time monitoring by observing residual energy level in the network; and (ii) total number of messages received successfully. Such an evaluation gives information about network performances using different link layer protocols as well as their energy consumptions. In order to get a clear demonstration of each protocol performance for different levels of ρ , results are plotted individually. The protocols provide performance increase by preserving energy and maintaining the nodes alive as much as possible. Frames are organized to be suitable for IPv6 where their sizes are fixed to 127 octets for IEEE 802.15.4, and 1280 octets for others using 6LoWPAN. Data link layer performance in the respect of received data size per a unit of transmission time (1 s) is experimentally obtained and illustrated by bar graphs given in Figs. 10–15. This illustration is made according to changes in ρ by figure by figure. In each figure, small (with 5 nodes), moderate (with 10 nodes), and dense (with 50 nodes) WPAN data throughputs are given in bars. To evaluate the impact of changing environmental conditions with variable ρ values, which is caused by mobility, we simulated the protocol operations in terms of data transmission rate using different channels with ρ ranging from 0% to 5% for peer to peer communications (Fig. 16). ADLL performance improvement on these ρ values are also given as factor values in Tables 10–12. A line graph showing changes in data throughput versus ρ for the moderate WPAN is plotted by Fig. 17. Performance change according

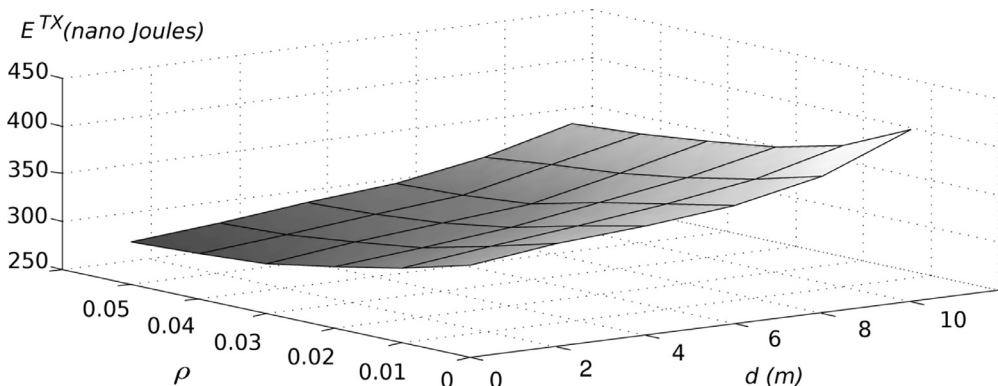


Fig. 9. Transmit energy consumption.

Table 8
Setup parameters.

Name	Description	Value
aMaxBE	Maximum back-off exponent	5
aMaxFrameRetries	Maximum number of retransmission	3
aUnitBackoffPeriod	Backoff period in symbols	20
MacWaitDuration	Maximum time for waiting ACK message in symbols	120
CCAPeriod	Channel listening time for CCA process in symbols	8
macMaxCSMABackoffs	Maximum number for channel access failure	4
macMinBE	Minimum number for back-off exponent	3
f	Carrier frequency	2.4 GHz
Mode	MAC operating mode	Contention based
Message size	Size of protocol-data-unit in application-layer	1 kbit

Table 9
Chip specific parameters.

Name	Description	Value
MacAckDuration	Transmission period for ACK message in symbols	12
PhyTXtoRXDuration	Mode transfer time from transmission to reception	192 μ s
PhyRXtoTXDuration	Mode transfer time from reception to transmission	192 μ s
PhyCCAtoTXDuration	Mode transfer time from channel listening to transmission	106 μ s

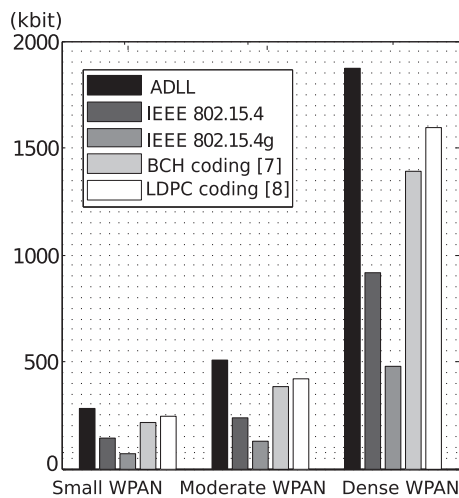


Fig. 10. Data gathering per second for $\rho \approx 0$.

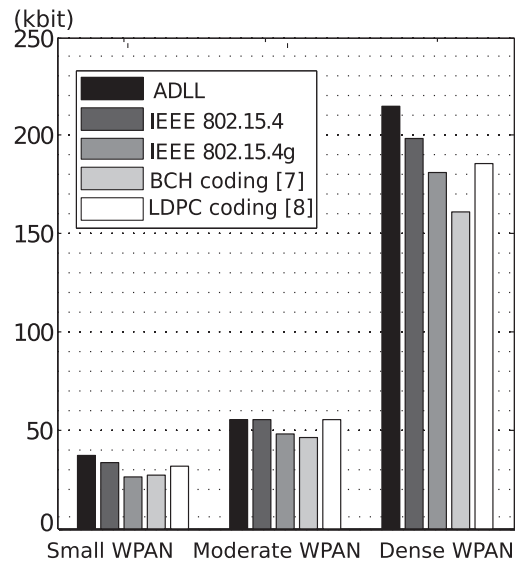


Fig. 12. Data gathering per second for $\rho = 0.02$.

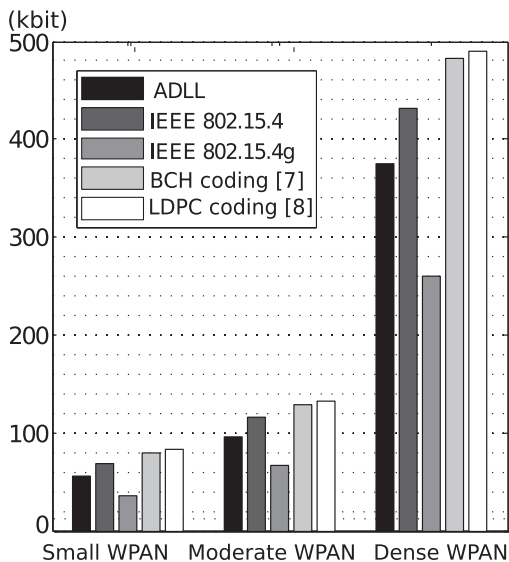


Fig. 11. Data gathering per second for $\rho = 0.01$.

to the different ρ values is clearly seen from this figure. The performance constantly degrades as the value of ρ gets higher. From the bar graphs, individual WPAN performance can be analysed. Fig. 10 shows where there is no error or very small amounts of error ($\rho \approx 0$). ADLL performs the best at this condition where the others follow as LDPC Coding [8], BCH Coding [7], IEEE 802.15.4g and IEEE 802.15.4. As ρ increases to 0.01 and closes to 0.02 (Figs. 11 and 12), the performance of ADLL decreases sharply. As environmental noise increases to higher levels causing ρ above 0.02 and 0.03, ADLL gets its superiority again (Figs. 12 and 13). In this condition, it is notable that the performance of LDPC Coding [8] gets closer to ADLL. However, as ρ increases to further values in [0.04,0.05], the success of LDPC Coding remains far below from ADLL as seen from Figs. 14 and 15. Performance factors for ADLL give a good comparison for the protocol outputs as given in Tables 10–12. The values in the tables are given by the ratios of successfully received data bits by ADLL to that of others. It is seen from the tables that ADLL performs about $\times 2$ factor when ρ is near 0 and over 0.04 for the most of its counterparts. When ρ gets values in [0.02,0.03], ADLL's success remains near $\times 1.5$ factor in average. However, when ρ closes to 0.01, its success falls sharply. ADLL performs

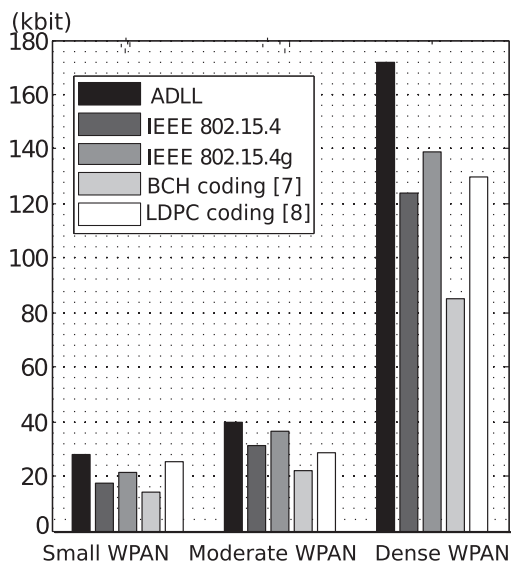


Fig. 13. Data gathering per second for $\rho = 0.03$.

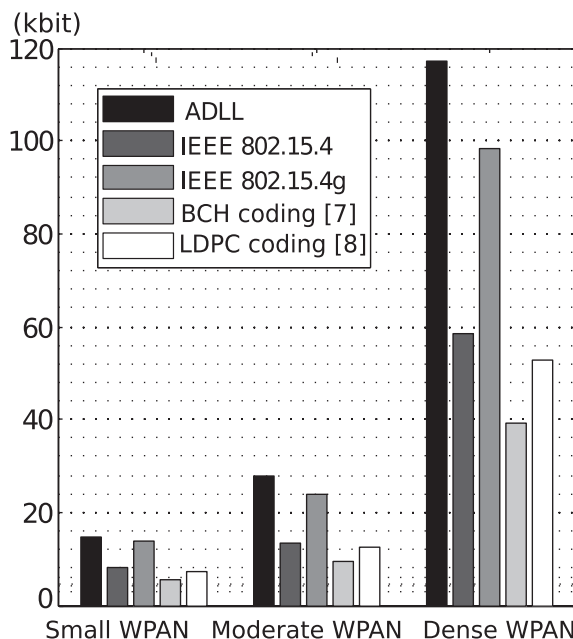


Fig. 15. Data gathering per second for $\rho = 0.05$.

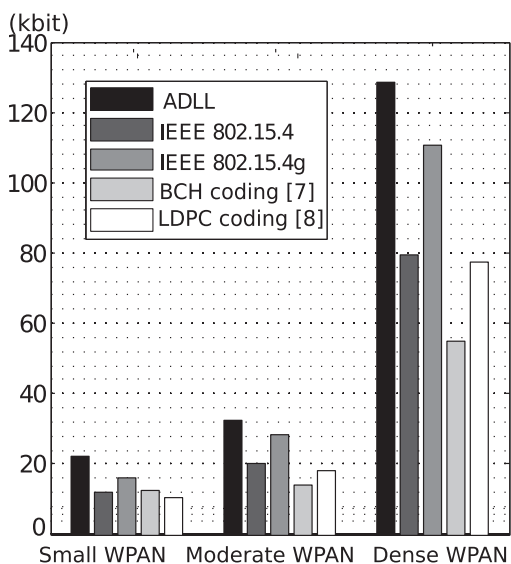


Fig. 14. Data gathering per second for $\rho = 0.04$.

Table 10 Performance factors of ADLL for the small WPAN.

ρ	IEEE 802.15.4	IEEE 802.15.4g	BCH coding [7]	LDPC coding [8]
≈ 0	1.99	3.82	1.31	1.14
0.01	0.81	1.51	0.69	0.66
0.02	1.09	1.39	1.34	1.17
0.03	1.59	1.28	1.96	1.09
0.04	1.85	1.35	1.79	2.12
0.05	1.79	1.06	2.63	1.99

Table 11 Performance factors of ADLL for the moderate WPAN.

ρ	IEEE 802.15.4	IEEE 802.15.4g	BCH coding [7]	LDPC coding [8]
≈ 0	2.12	3.95	1.32	1.20
0.01	0.83	1.43	0.75	0.73
0.02	1.00	1.15	1.21	1.01
0.03	1.27	1.10	1.81	1.39
0.04	1.60	1.13	2.28	1.76
0.05	2.05	1.16	2.98	2.18

Table 12 Performance factors of ADLL for the dense WPAN.

ρ	IEEE 802.15.4	IEEE 802.15.4g	BCH coding [7]	LDPC coding [8]
≈ 0	2.03	3.88	1.35	1.18
0.01	0.87	1.44	0.78	0.77
0.02	1.08	1.19	1.34	1.16
0.03	1.38	1.23	2.02	1.32
0.04	1.61	1.16	2.33	1.66
0.05	2.00	1.19	2.98	2.22

greater amount of data gathering for the most of ρ values in $[0,0.5]$. Its weak performance is observed when ρ is valued about 0.01. The performance at this level decreases considerably. However, ADLL performance for other ρ values can be reached to the value over 200% comparing to the closest performance.

It is notable for IEEE 802.15.4 protocol that it keeps its resilience to noise signals up to very high levels (Fig. 17). The superiority of its resilience over IEEE 802.15.4g begins after 2.5% of the bit error rate. Its high resilience is provided by keeping its spreading factor at a high

level which is given as 8 with DSSS(32,4). However, this level is too high for low ρ values causing decline in data transmission rate. This is observed at the level of about $\times 0.5$ factor in throughput (where ρ is about 0.5%). As seen from Fig. 17, it is notable that IEEE 802.15.4 has a robust response to ρ values in the given range. This robustness is provided by its high spreading factor by DSSS(32,4). By contrast, such a factor causes throughput to be decreased significantly over the whole range of ρ . On the other hand, IEEE 802.15.4g and ADLL respond to the changes in ρ by more gradient values. This condition is mostly observed in $[0,0.02]$ of ρ values. However, IEEE 802.15.4 performs less performance than IEEE 802.15.4g up to the value of 0.025 of ρ , and than ADLL for all the range of ρ . It is clear from the figure that ρ has an enormous influence on the throughput. The numerical results show that an appropriate frame organization with ADLL maximizes the mean value of throughput for a wide range of ρ .

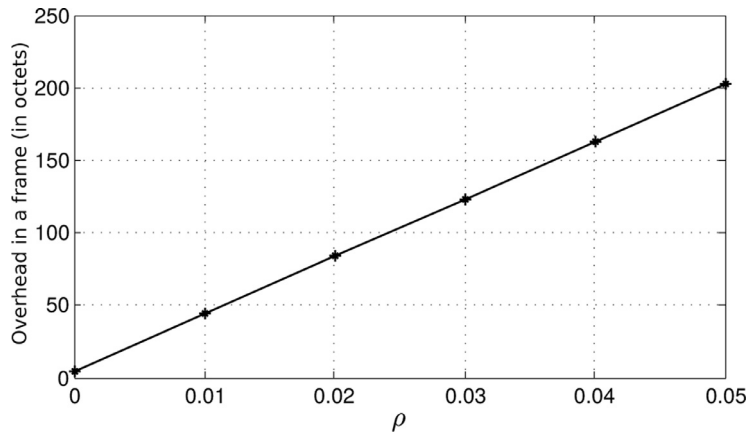


Fig. 16. Transmission overhead versus ρ .

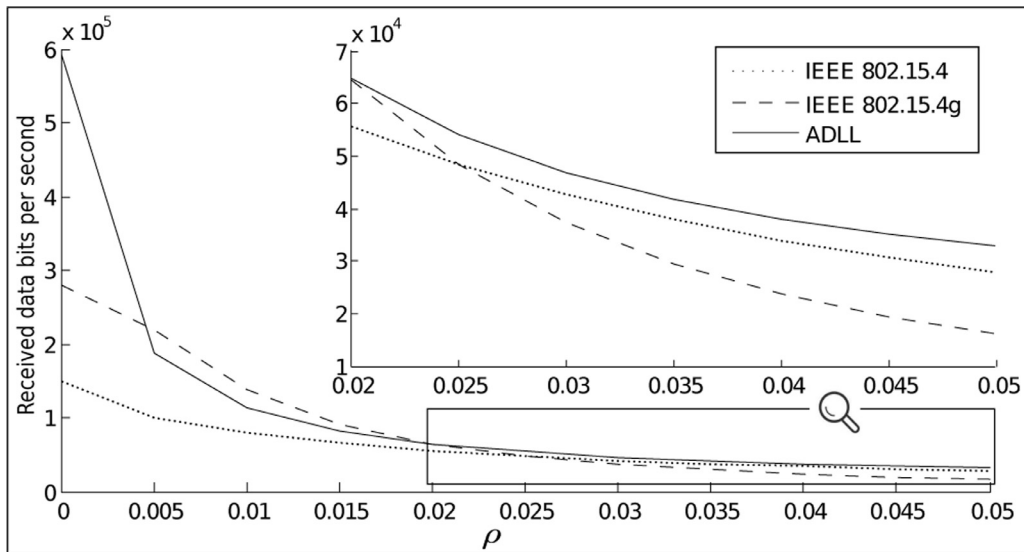


Fig. 17. Throughputs of the protocols.

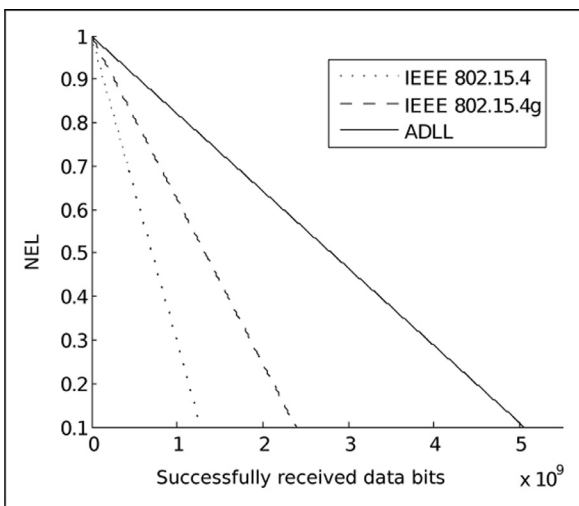


Fig. 18. NEL versus received data bits with $\rho \approx 0$.

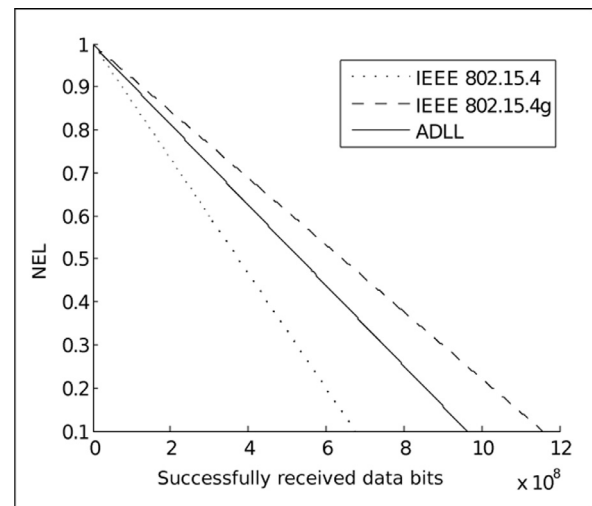
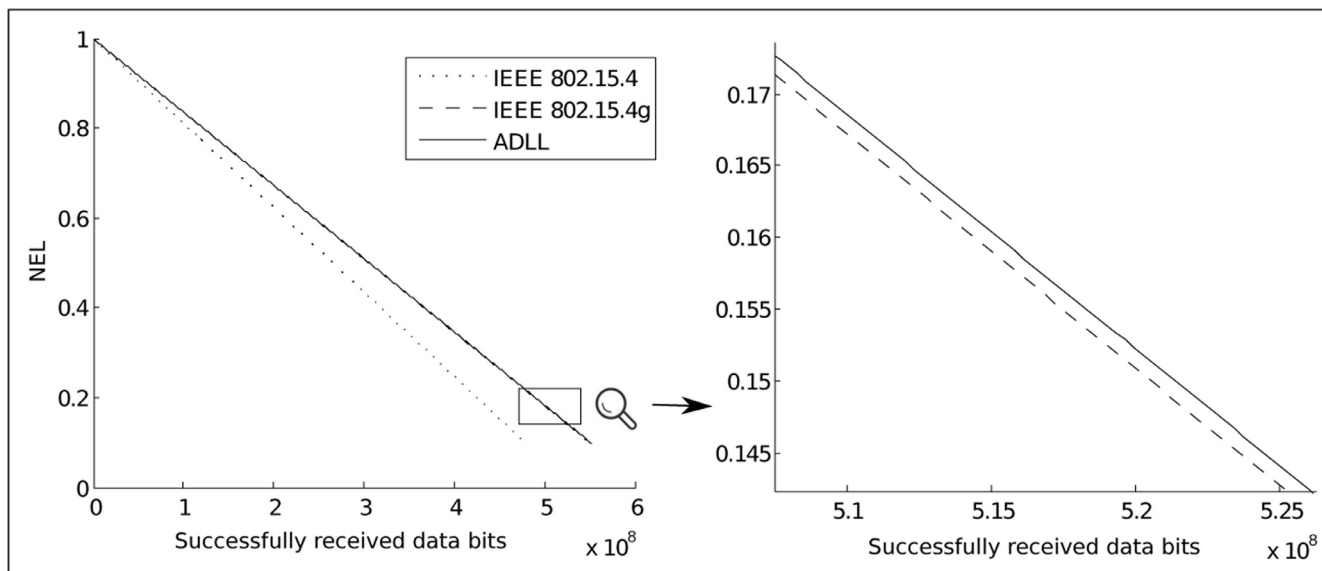
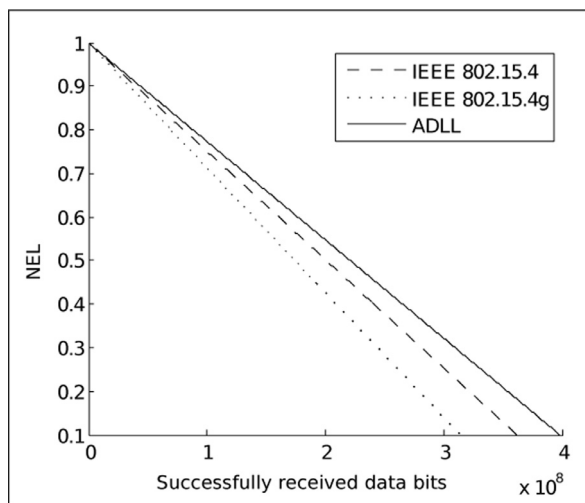
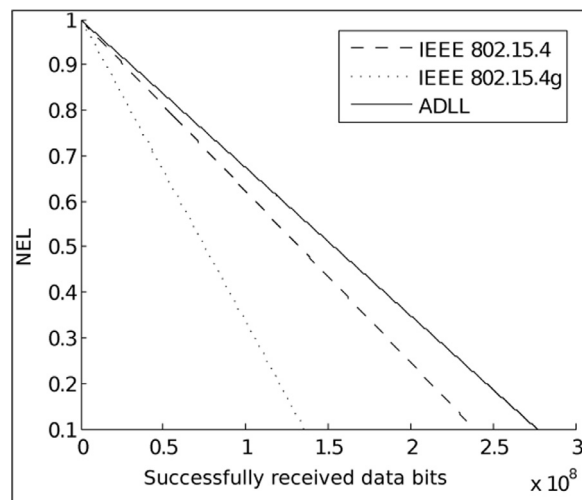
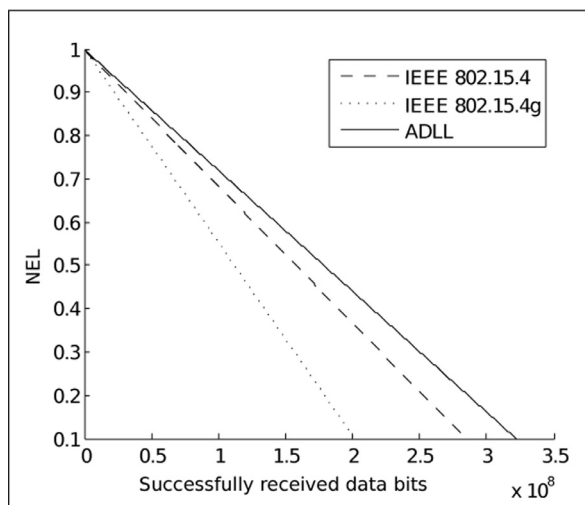


Fig. 19. NEL versus received data bits with $\rho = 0.01$.

Fig. 18 shows that no environmental noise is present or near ideal condition is met by near zero values of ρ . Differences in data gathering performances are clearly seen where network energy closes to be emptied. ADLL offers its highest performance where ρ is

extremely small. It succeeds to receive over $5.06 \cdot 10^9$ data bits while IEEE 802.15.4g and IEEE 802.15.4 receive below $2.38 \cdot 10^9$ and $1.28 \cdot 10^9$ data bits, respectively. ADLL has its lowest performance where ρ is valued by 0.01 as shown in Fig. 19. Decrease in the performance at

Fig. 20. NEL versus received data bits with $\rho = 0.02$.Fig. 21. NEL versus received data bits with $\rho = 0.03$.Fig. 23. NEL versus received data bits with $\rho = 0.05$.Fig. 22. NEL versus received data bits with $\rho = 0.04$.

this value observed as 20% comparing to that of IEEE 802.15.4g. However, it performs about 40% more performance than IEEE 802.15.4. When ρ is valued by 0.02, outputs are observed at close values to each-other as shown in Fig. 20. It is notable that IEEE 802.15.4 brings much more performance decrease as network energy depletes while ADLL performs the best performance. The performance difference between IEEE 802.15.4g and ADLL gets a clearer view while the energy closes to the end. Superiority of ADLL is also observed in wireless channels with ρ values of 0.03, 0.04, and 0.05 as shown in Figs. 21–23. It is observed from these figures that IEEE 802.15.4 gets more performance than IEEE 802.15.4g with ρ values over 0.025. From these observations, it can be concluded that IEEE 802.15.4 provides better performance than IEEE 802.15.4g for ρ values over 0.025. However, ADLL performs the best performance for all ρ values except 0.01.

The states of ADLL algorithm (Fig. 5) can be employed by the processor of a transceiver module in real-time. To make its complexity analysis, the functions and related routines of the states are compiled by means of GNU C++ compiler and its library file (math.h). After compilation, the program is embedded to processors which are well-known for real-time applications [21]. The operation requires 136 machine level instructions to employ an ADLL frame. The

Table 13
Operational specifications of ADLL.

Processor unit	ARM Cortex-M0	ARM Cortex-M3
MIPS	127 MIPS at 50 MHz	378 MIPS at 100 MHz
Operating power	5.1 μ W/MHz (255 μ W at 50MHz)	8 μ W/MHz (800 μ W at 100 MHz)
Execution time(s)	$1.07 \cdot 10^{-6}$	$3.60 \cdot 10^{-7}$
Required energy(pJ)	273.07	287.83

processors, clock frequencies, Mega Instruction Per Second (MIPS) values, execution times, and required energies are given in Table 13. These values give information about time complexities of ADLL operation and its energy requirement. As seen from the table, execution of ADLL job by the proposed chips requires very small time periods comparing to a unit of back-off time (320 ms) of IEEE 802.15.4 communications. It is also notable that the computations require as low energy as about a thousand times smaller than transmission energy (Fig. 9). Computational energy requirement turns relatively small amounts of battery consumption which can be negligible.

ADLL has the same control fields as in IEEE 802.15.4 and IEEE 802.15.4g. However, it uses more additional control fields to provide higher resilience for noisy communications. These fields are given as block CRCs, LQ, and erroneous block IDs. Block CRCs are used in general data frames. And, the others are used for ACK frames. The operations of these fields are described in Section 4. From the performance simulations, transmission overhead of these fields are observed as given in Fig. 16. However, this overhead is bearable as it eventually returns high resilient transmissions, providing high data throughputs, as discussed in the evaluation of performance.

6. Conclusions

WPANs are emerging technologies for short-range communications to be used in computer, industrial, and many control systems. Low-powered and low-rate WPAN communication is standardized by the IEEE 802.15 working group in 2003. The standard specifies the physical layer and link layer operations. It is commonly used in many applications. In 2012, the standard is improved as IEEE 802.15.4g. Although this newer version of the standard has many advantages over its predecessor, adaptation issues to mobile conditions are not discussed by its specifications. Since, mobile conditions cause physical parameters to be in changing values, physical from/to link layer interactions are essential to provide an optimum operation. In this paper, a comprehensive study of WPAN architecture for cross-layer cooperation has been conducted. The objectives of new low-power WPAN communication paradigms have been described. Also, the proposed protocol operations for this type of networks are explained in detail. Then, its performance over IEEE protocols is investigated for various environmental conditions. Link-layer performance of the proposed method is analysed for mobile conditions. This analysis is made by observing Monte Carlo (MC) simulations for the environments with various bit error rates. Performance results are compared with IEEE 802.15.4 and IEEE 802.15.4g which are commonly used protocols in low-rate and low-power wireless networks. Energy consumptions of battery powered LR-WPAN networks are analysed for each protocol and MC simulations are made to observe network life-time in a comparative way. Comparisons show that the proposed method provides low-cost, low-energy consumption, and high throughput. These

features offer advantageous solutions to WPANs to be more powerful and functional in low-power operations.

References

- [1] A. Bensky, *Short-range Wireless Communication*, 2nd edition, Newnes Press, MA, USA, 2004.
- [2] IEEE P802.15 Working Group, IEEE std. 802.15.4-2003, part. 15.4: Wireless Medium Access Control (MAC) and Physical Layer (PHY) Specifications for Low-Rate Wireless Personal Area Networks (LR-WPANs), Technical Report, IEEE, New York, NY 10016-5997, USA, 2003.
- [3] IEEE P802.15g Working Group, IEEE std. 802.15.4g, part. 15.4: Amendment 3: Wireless Medium Access Control (MAC) and Physical Layer (PHY) Specifications for Low-Rate Wireless Personal Area Networks (LR-WPANs), Technical Report, IEEE, New York, NY 10016-5997, USA, 2012.
- [4] G. Mulligan, The 6LoWPAN architecture, in: *Proceedings of the 4th Workshop on Embedded Networked Sensors, EmNets'07*, New York, NY, U.S.A., 2007, pp. 78–82.
- [5] J. Misić, S. Shafi, V. Misić, The impact of MAC parameters on the performance of 802.15.4 PAN, *Ad Hoc Netw.* 3 (2005) 509–528.
- [6] J. Zhu, Z. Tao, C. Lv, Performance evaluation for a beacon enabled IEEE 802.15.4 scheme with heterogeneous unsaturated conditions, *Int. J. Electron. Commun.* 66 (2012) 93–106.
- [7] B. Shen, A. Abedi, A simple error correction scheme for performance improvement of IEEE 802.15.4, in: *Proceedings of USAIEEE LCN02 International Conference on Wireless Networks*, Las Vegas, Nevada, U.S., 2007, pp. 387–393.
- [8] A. Biroli, M. Martina, G. Masera, An LDPC decoder architecture for wireless sensor network applications, *Sensors* 12 (2) (2012) 1529–1543.
- [9] N. Javaida, et al., AID: an energy efficient decoding scheme for LDPC codes in wireless body area sensor networks, *Proc. Comput. Sci.* 21 (2013) 449–454.
- [10] M. Hefeida, T. Canli, A. Khokhar, CL-MAC: a cross-layer MAC protocol for heterogeneous wireless sensor networks, *Ad Hoc Netw.* 11 (2013) 213–225.
- [11] T. Beluch, D. Dragomirescu, R. Plana, A sub-nanosecond synchronized MAC PHY cross-layer design for wireless sensor networks, *Ad Hoc Netw.* 11 (2013) 833–845.
- [12] J. Montavont, D. Roth, T. Noel, Mobile IPv6 in internet of things: analysis, experiments and optimizations, *Ad Hoc Netw.* 14 (2014) 15–25.
- [13] V. Guruswami, *Introduction to Coding Theory*, Notes 1: Introduction, Linear Codes, Technical Report, Computer Science Dept., Carnegie Mellon University, Gates-Hillman Complex 7211, 2010. Carnegie Mellon University, 5000 Forbes Avenue Pittsburgh PA 15213, USA
- [14] C. Kelley, *SIAM Frontiers in Applied Mathematics*, vol. 18, Society for Industrial and Applied Mathematics, North Carolina, U.S.A., 1999.
- [15] J. Hui, P. Thubert, Compression format for IPv6 datagrams over IEEE 802.15.4-based networks, request for comments (RFC) 6282 Tech. rep., 2011, Internet Engineering Task Force (IETF), LLC (AMS) 48377 Fremont Blvd., Suite 117, Fremont, California 94538, USA.
- [16] W.H. Press, S.A. Teukolsky, W.T. Vetterling, B.P. Flannery, *Numerical Recipes: The Art of Scientific Computing*, 3rd edition, Cambridge University Press, NY, USA, 2007.
- [17] E.A.V. Kapnadak, Distributed iterative quantization for interference characterization in wireless networks, *Digit. Signal Process.* 22 (1) (2012) 96–105.
- [18] A.D.T.S. Center, 2015, Low Power IEEE 802.15.4 Zero-IF 2.4 GHz Transceiver IC, Technical Report, Analog Devices Inc., One Technology Way, P.O. Box 9106, Norwood, MA 02062-9106, U.S.A. Available online at: www.analog.com/media/en/technical-documentation/data-sheets/ADF7241.pdf.
- [19] L. Bajaj, et al., *GloMoSim: A Scalable Network Simulation Environment*, Technical Report, Computer Science Dept., University of California, Los Angeles, USA, 1999.
- [20] G.R. Group, 2014, CR1216 Battery Catalog, Technical Report, GP Batteries Int. Ltd.; GPI International Ltd., Singapore. Available online at: www.gpbatteries.com/INT/images/prod/.
- [21] ARM Technical Support Team, 2015, Cortex-M Series, Technical Report, ARM Ltd., 110 Fulbourn Road. Cambridge. GB. Available online at: www.arm.com/products/processors/cortex-m/.